RESEARCH PAPER

Channels 9:1, 30–43; January/February 2015; © 2015 Taylor & Francis Group, LLC

A long isoform of the epithelial sodium channel alpha subunit forms a highly active channel

Jonathan M Berman, Cristin Brand, and Mouhamed S Awayda*

Department of Physiology and Biophysics; State University of New York at Buffalo; Buffalo, NY USA

Keywords: alternative splicing, electrophysiology, epithelial sodium channel (ENaC), hypertension, ion channels, protease

A long isoform of the human Epithelial Sodium Channel (ENaC) α subunit has been identified, but little data exist regarding the properties or regulation of channels formed by α_{728}. The baseline whole cell conductance of oocytes expressing trimeric $\alpha_{728}\beta\gamma$ channels was 898.1 ± 277.2 and 49.59 ± 13.2 μS in low and high sodium solutions, respectively, and was 11 and 2 fold higher than the conductances of $\alpha_{669}\beta\gamma$ in same solutions. $\alpha_{728}\beta\gamma$ channels were also 2 to 5 fold less sensitive to activation by the serine proteases subtilisin and trypsin than $\alpha_{669}\beta\gamma$ in low and high Na^+ conditions. The long isoform exhibited lower levels of full length and cleaved protein at the plasma membrane and a rightward shifted sensitivity to inhibition by increases of $[Na^+]_i$. Both channels displayed similar single channel conductances of 4 pS, and both were activated to a similar extent by reducing temperature, altogether indicating that activation of baseline conductance of $\alpha_{728}\beta\gamma$ was likely mediated by enhanced channel activity or open probability. Expression of α_{728} in native kidneys was validated in human urinary exosomes. These data demonstrate that the long isoform of αENaC forms the structural basis of a channel with different activity and regulation, which may not be easily distinguishable in native tissue, but may underlie sodium hyperabsorption and salt sensitive differences in humans.

Introduction

Background

Hypertension is a risk factor for myocardial infarction and stroke. One of the primary determinants of an individual's blood pressure is blood volume, which is chronically regulated by the kidneys. Reabsorption of water from the nephron lumen to the plasma is tied to the osmotic gradient created by the movement of sodium. The epithelial sodium channel (ENaC) is the final step in sodium reabsorption in the collecting duct of the nephron (CD) and the rate-limiting step in reabsorption in these epithelia.

High activity ENaC is a heteromultimer consisting of a structural subunit, typically α, as well as β and γ subunits with a membrane stoichiometry which electrophysiology indicates consists of 2 α subunits, one β and one γ,[1] while structural homology to the crystalized acid sensing ion channel (ASIC),[2,3] suggests a trimer of each subunit.

Modularity and alternate splicing

α ENaC is critical for channel formation.[1,4] α-like subunits such as *Xenopus* epsilon,[5] ASIC1,[6] or human δ, can exhibit different properties and may substitute for α in some tissues yielding channels with different activity and/or regulation. In humans, a longer α isoform has been detected in the kidney but it remains incompletely characterized.[7] We examined the properties of this 728 a.a isoform because little is known about its physiological function and regulation despite being first identified by Thomas et al. in 1998 where it was shown to have single channel conductance and macroscopic currents similar to those of the 669 a.a. isoform. It was also shown to be expressed in multiple tissues including colon, lung, and kidney,[7] however, there are no detailed comparisons between channels formed with α_{728} and α_{669}.

A significant part of ENaC regulation occurs through membrane trafficking/recycling leading to differences of membrane protein expression.[8] Another major aspect of regulation occurs through changes to open probability mainly through proteolytic cleavage of the channel.[9] The channel also responds to changes of intra and extracellular Na^+ leading to downregulation in response to increases of $[Na^+]$.[10,11] The response and regulation of α_{728} channel by $[Na^+]$ is undetermined and is examined in the current work.

Regulation by $[Na^+]$ and proteolysis

Two types of inhibition by sodium have been described and differentiated based on time course:[12-14] a slow effect due to high $[Na^+]$, termed "feedback inhibition," and mediated by PKC[15] and a fast effect termed "self-inhibition" likely mediated by the Na^+ ions interaction with the channel,[11] and this represents an intrinsic channel property that does not require further second messenger.[14] ENaC in native epithelia, and especially in the kidney, is exposed to different $[Na^+]$ making both regulatory processes physiologically relevant. Further, there is variation in the degree to which blood pressure is sensitive an individual's salt intake, and it is unknown if such differences could be, at least in part, mediated by differences in the structural isoform expressed (α_{669} vs α_{728}).

*Correspondence to: Mouhamed S Awayda; Email: awayda@buffalo.edu
Submitted: 10/21/2014; Revised: 10/31/2014; Accepted: 11/04/2014
http://dx.doi.org/10.4161/19336950.2014.985478

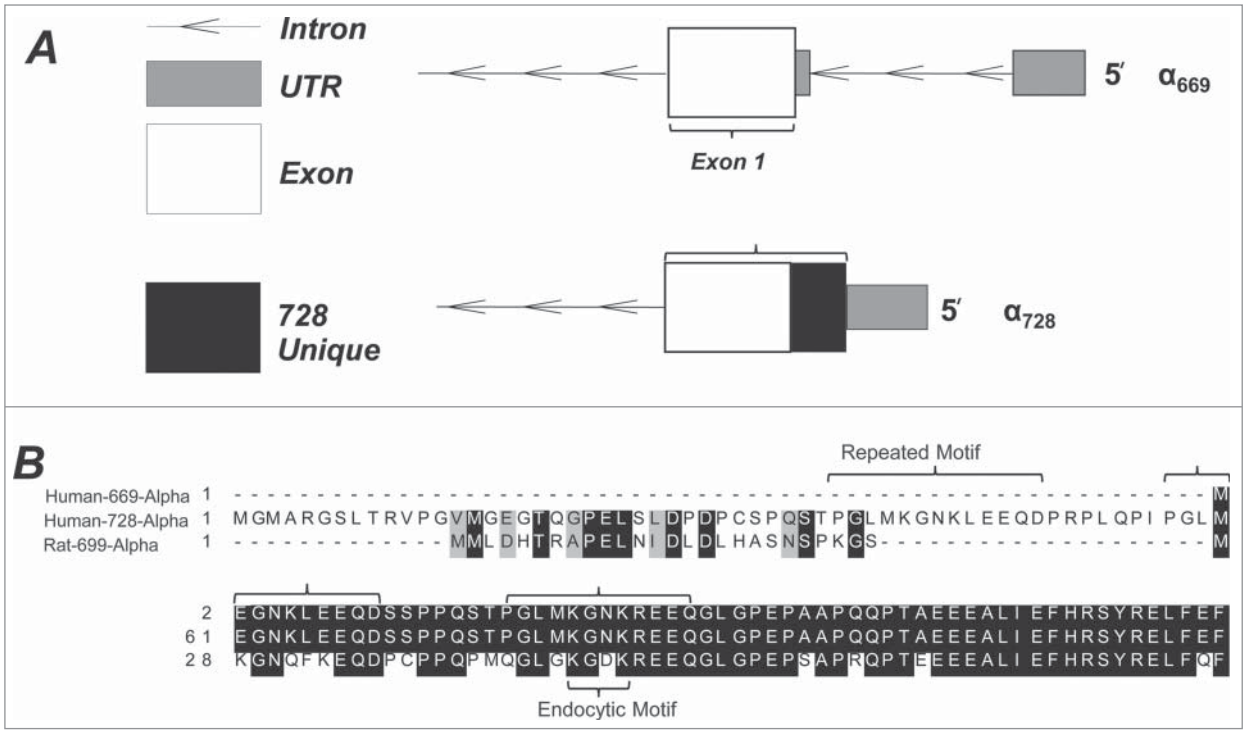

Figure 1. Layout of the N-terminus of human α ENaC. Two isoforms are described with a conventional form resulting in 669 a.a. and an alternative longer N-terminus form resulting in a 728 a.a. (**A**) The coding sequence organization in α_{728} is similar to that of α_{669} with the exception of a different 5′ UTR and a different exon 1 start site resulting in 59 unique a.a. Figure generated in FancyGene.[47] (**B**) A multiple sequence alignment of the 1st 61 a.a. of α_{728} showing homology to the first 26 a.a. of rat α ENaC, as well as a repeating motif, which contains a smaller motif homologous to an endocytic domain identified in rENaC.[48]

Another regulator of channel activity is cleavage by internal and external proteases.[9,16,17] This occurs on two ENaC subunits, with α being one of these subunits.[9] Cleavage markedly increases open probability (P_o) either by removal of an inhibitory tract,[18] or loss of the first transmembrane domain.[19] The baseline intracellular and exogenous extracellular cleavage of channels formed with α_{728} by proteases is unknown. Given the chronic exposure of ENaC to urinary proteases, differences in proteolytic activation of these subunits is of potential significance to renal sodium handling in the CD.

Effects of temperature

In addition to the above processes, ENaC is stimulated by membrane rigidification by cooling.[20,21] This effect increases channel P_o possibly by increased membrane order and rigidity and interaction with the lipid bilayer.[20] This activation of P_o is likely separate from that caused by cleavage, as it is immediate and reversible, and, it is unknown if the 2 human α isoforms exhibit similar responses to cooling.

We report that $\alpha_{728}\beta\gamma$ forms a high activity channel despite low plasma membrane density of the full length and cleaved forms. This indicates that ENaC may be highly active in the absence of cleavage. Regulation by Na^+ was also different with α_{728} channels exhibiting larger inhibition by chronic and acute high $[Na^+]_i$ with sensitivity shifted to higher $[Na^+]$. Effects of temperature were similar indicating that the interaction with the lipid bilayer was not likely modified. Altogether, these data indicate that α_{728} can form a high activity channel *in vivo* that is less dependent on proteolysis for its activity and is further stimulated in low $[Na^+]_i$, and that the existence of channels with this isoform may predispose collecting duct epithelia to Na^+ retention.

Results

Structure and function

The structure and function of the α ENaC N-terminus remains largely unstudied despite being 1st identified by Thomas and colleagues in 1998.[7] We examined the amino acid sequence of the extended α_{728} N-terminus with to the known α_{669} sequence and homology to rat. **Figure 1A** represents the alternative splice sites which give rise to the differences in the mRNA sequence between α_{669} and α_{728}. The α_{728} transcript produces upstream an additional 59 amino acids from a longer first exon of α_{669} which also contains a unique 5′ UTR. Because the ASIC structure solved by Jasti et al.[2] did not include the N-terminus there is no homologous structure to which this sequence can be compared to estimate a secondary structure.

We compared the human α_{728} sequence to that of rat α_{699} (**Fig. 1B**) because the rat N-terminus is longer than that of human α_{669} and because there are notable electrophysiological differences between rat and human ENaC especially in terms of voltage activation and sensitivity to Na^+.[22] The first 24 a.a. of the rat sequence

are homologous to human α_{728} a.a 13-37, and these are absent from the human α_{669} sequence.

Rectification and voltage activation

Two of the characteristic electrophysiological properties of $\alpha_{669}\beta\gamma$ are its current-voltage relationship which shows inward rectification (**Fig. 2**), and a voltage dependent activation possibly by voltage induced changes to $[Na^+]$ at the inner mouth of the channel.[22] Rectification and voltage activation are in addition to Na^+-self inhibition intrinsic channel properties and changes in them reflect differences in channel properties and function. We tested rectification and voltage activation of $\alpha_{728}\beta\gamma$ to determine if the longer N-terminus led to differences in these properties.

Rectification of the $\alpha_{728}\beta\gamma$ and $\alpha_{669}\beta\gamma$ channels was assessed from the ratio of the slope conductances at −100 mV and +40 mV in ND94 recording solution. Conductance of $\alpha_{728}\beta\gamma$ (**Fig. 2**) was more linear (1.68 ± 0.21) than $\alpha_{669}\beta\gamma$ (5.47 ± 0.81) at hyperpolarizing voltages (**Fig. 2D**, $P < 0.01$).

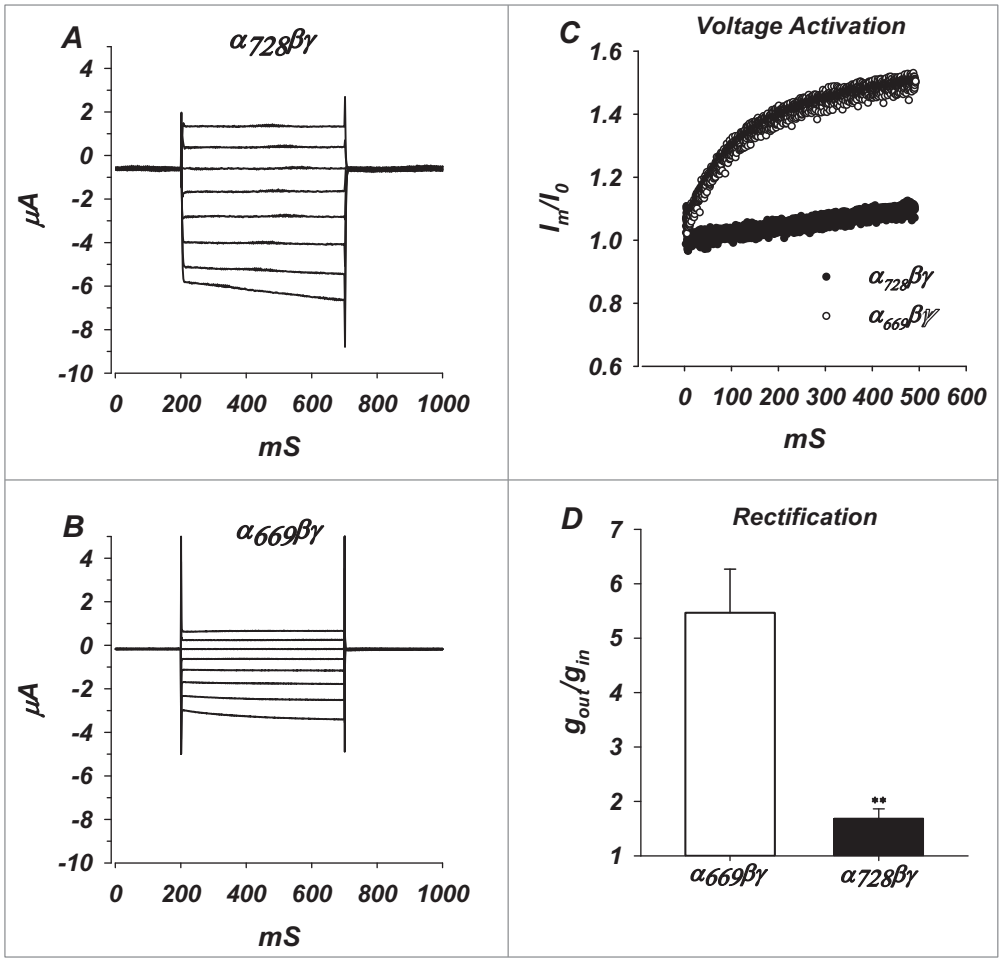

Figure 2. Whole cell currents, voltage activation and rectification of $\alpha_{728}\beta\gamma$ channels. (**A**) Whole cell currents of $\alpha_{728}\beta\gamma$ in the voltage range of −100 to +40 mV. (**B**) Whole cell currents of $\alpha_{669}\beta\gamma$. (**C**) Normalized currents at −100 mV, demonstrating voltage activation and differences between the 2 isoforms (n = 6, $P < 0.05$). I_o represents the current immediately after voltage clamping. (**D**) Comparison of the ratio of outward to inward slope conductances indicating larger inward rectification of α_{669} channels. n = 11 and 25 for α_{669} and α_{728}. ** denote $P < 0.01$.

Voltage dependent activation at −100 mV in $\alpha_{728}\beta\gamma$ was apparently less than that observed in $\alpha_{669}\beta\gamma$. The observed activation in $\alpha_{728}\beta\gamma$ was longer than the 500 ms measurement and for this reason it was not possible to determine a finite time constant or magnitude of activation (**Fig. 2C**). Therefore, we cannot rule out that the reduced activation is actually just due to a much longer time constant of activation of $\alpha_{728}\beta\gamma$. Given complications with Na^+ loading in prolonged clamping to −100 mV, it was not possible to extend the time course of the measurement to accurately obtain a time constant. Nonetheless, these data indicate marked differences in the way these 2 channels respond to acute changes of voltage.

These differences of voltage activation and rectification led to a different characteristic I/V relationship for the 2 isoforms. Consistent with effects of Na^+ and voltage on these parameters, we expect that these isoforms would also exhibit different responses to changes of $[Na^+]$.

Whole cell conductance

Thomas et al.[7] reported similar macroscopic currents between $\alpha_{669}\beta\gamma$, and $\alpha_{728}\beta\gamma$. However, their experiments were designed to examine if channels containing α_{728} were largely similar to those containing α_{669}. Recordings were also performed under high sodium conditions, which could miss some of the differences between these 2 isoforms by different $[Na^+]_i$. To further explore these differences, especially in light of differences in rectification and voltage activation, we tested the baseline activity of both isoforms under chronic conditions of high or low $[Na^+]$.

Incubation of ENaC expressing oocytes in low extracellular Na^+ reduces $[Na^+]_i$ from 65 mM to 12 mM. As seen in **Figure 3A**, $\alpha_{728}\beta\gamma$ oocytes incubated in low Na^+ had a baseline amiloride sensitive conductance (g_{Na}) of 898.1 ± 277.2 μS (n = 13), while $\alpha_{669}\beta\gamma$ injected oocytes had a baseline conductance of 49.59 ± 13.2 μS (n = 13). This 18 fold difference indicates marked differences in overall activity between the 2 constructs caused by the extended N-terminus.

Higher activity of $\alpha_{728}\beta\gamma$ persisted in high Na^+, however, prolonged incubation in the 96 mM Na^+ solution lead to larger decrease of the g_{Na} of $\alpha_{728}\beta\gamma$ relative to that of $\alpha_{669}\beta\gamma$, which

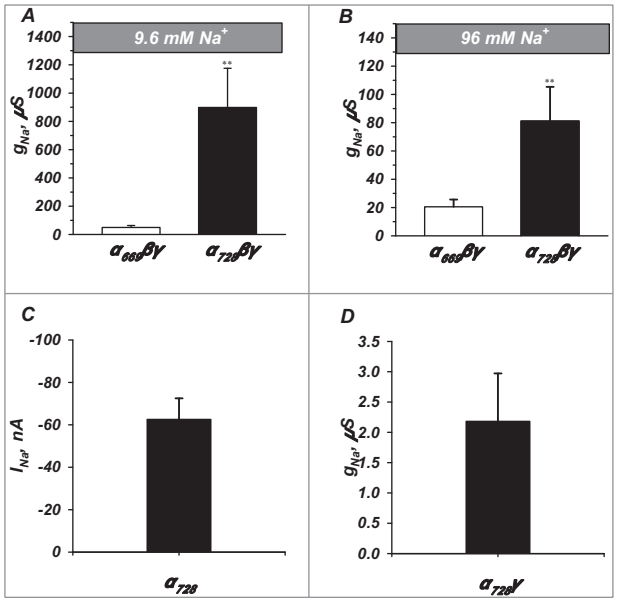

Figure 3. $\alpha_{728}\beta\gamma$ forms a high activity channel. Channel activity was examined under both low (9.6 mM) and high (96 mM) Na^+ and with different subunit combinations. $\alpha_{728}\beta\gamma$ exhibited appreciably higher activity than $\alpha_{669}\beta\gamma$ in both low (**A**) and high (**B**) Na^+ conditions although the magnitude of the differences were larger in low Na^+ (n = 13-24). (**C and D**) α_{728} did not efficiently form channels in the absence of β and γ or in the absence of β (n = 20-7). ** denote $P < 0.01$.

decreased to 81.1± 24.2 μS (n = 23) and 20.5± 5.1 μS (n = 24), respectively. Thus, high Na^+ caused an additional 4.5 fold inhibition of $\alpha_{728}\beta\gamma$ relative to $\alpha_{669}\beta\gamma$ (11 vs 2.5 fold inhibition of $\alpha_{728}\beta\gamma$ versus $\alpha_{669}\beta\gamma$). This indicates that $\alpha_{728}\beta\gamma$ inhibition by increasing $[Na^+]_i$ requires higher values which are greater than 12 mM and in the range of 65 mM; or that $\alpha_{669}\beta\gamma$ is more sensitive to $[Na^+]_i$ and is already inhibited to a larger extent than $\alpha_{728}\beta\gamma$ in the range of 12 mM.

The activity of channels formed by α ENaC is heavily dependent on the co-expression of the β and γ subunits. To eliminate the possibility that α_{728} is capable of forming highly active channels alone or under different subunit combinations we expressed only α_{728} and in combination with γ in absence of the β subunit. On its own, the conductance of α_{728} was too low to be accurately measured and it displayed a current at −100 mV of 62.6± 9.9 nA (**Fig. 3C**). Channels formed with $\alpha_{728}\gamma$ had an amiloride sensitive conductance of 2.2± 0.7 μS indicating that all 3 subunits are required for full activity and that the extended N-terminus does not change this requirement.

Activation by proteases

Proteolysis is a major regulatory mechanism for ENaC, having been observed *in vivo* and *in vitro*. This process is also known to be reproduced in the oocyte system. Because α_{728} has been detected in the kidney[7] (see below), and because endogenous urinary serine proteases can cleave and activate $\alpha_{669}\beta\gamma$ ENaC, we measured the proteolytic activation profiles of $\alpha_{669}\beta\gamma$ and $\alpha_{728}\beta\gamma$. We examined 2 serine proteases-trypsin and subtilisin-which have been shown to activate $\alpha_{669}\beta\gamma$.[17,19] As the data shown above suggested different responses to Na^+ between isoforms, we tested the effects of these proteases under both high and low Na^+ conditions.

A representative activation of $\alpha_{728}\beta\gamma$ with 50 ng/ml trypsin in high $[Na^+]$ is shown in **Figure 4A**. Trypsin caused a 15 fold activation in a time course similar to that we previously described for $\alpha_{669}\beta\gamma$.[9] In contrast, activation of channels formed with α_{728} and $\alpha_{728}\gamma$ alone (**Fig. 3B**) were minimal and ~2 fold or less indicating that this process-just like in α_{669}-required the presence of all 3 channel subunits.

In high $[Na^+]$ conditions subtilisin activated trimeric $\alpha_{669}\beta\gamma$ by 6.9± 2.2 fold, and $\alpha_{728}\beta\gamma$ by 2.0± 0.3 fold (**Fig. 4C**, $P < 0.05$). Activation in low $[Na^+]$ was 2.1 ± 0.4 fold for $\alpha_{669}\beta\gamma$ and 1.3± 0.2 fold for $\alpha_{728}\beta\gamma$ (**Fig. 4D**, $P < 0.05$). These data indicate interaction between $[Na^+]_i$ and proteolytic activation-a likely effect on baseline channel open probability (P_o). It also indicates that $\alpha_{728}\beta\gamma$ in low $[Na^+]_i$ is either nearly insensitive to proteolysis or that it is largely already cleaved by endogenous intracellular proteases. This was tested with a different protease.

Activation by trypsin followed a similar profile, but with larger magnitudes of activation. In high sodium trypsin activated $\alpha_{669}\beta\gamma$ by 53.6± 19.6 fold, and $\alpha_{728}\beta\gamma$ by 10.7 ± 2.7 fold (**Fig. 4E**, $P < 0.05$). In low sodium trypsin activated $\alpha_{669}\beta\gamma$ by 9.5 ± 2.8 fold, and $\alpha_{728}\beta\gamma$ by 2.9 ± 0.4 fold (**Fig. 4F**, $P < 0.05$). Thus, for both proteases activation of $\alpha_{728}\beta\gamma$ was lower in low Na^+ and less than that of $\alpha_{669}\beta\gamma$.

Protein expression and processing

In addition to intrinsic changes to channel function, changes in trafficking to or from the membrane and high membrane expression could explain the high activity seen in $\alpha_{728}\beta\gamma$. High endogenous cleavage could also explain the high baseline activity and low activation by external proteases. We tested both of these possibilities by biochemically examining channel plasma membrane expression and the magnitude of endogenous intracellular proteolytic processing. Given the marked differences in activation between high and low Na^+ we examined these parameters under both $[Na^+]_i$ conditions.

Western blot of oocytes expressing channels of either isoform in high or low sodium or α_{728} alone is shown in **Figure 5**. The longer α_{728} isoform in $\alpha_{728}\beta\gamma$ channels migrated at 88.1 ± 2.2 kDa while α_{669} in $\alpha_{669}\beta\gamma$ channels migrated at 81.6 ± 1.6 kDa. This is consistent with the presence of the additional 59 a.a. Both isoforms exhibited an endogenously cleaved form which migrated at 64.6± 1.8 and 60.9± 1.0 kDa, respectively.

The longer α_{728} isoform in trimeric channels exhibited low membrane and endogenous cleavage levels in both low and high Na^+. In this example α_{728} also exhibited lower intracellular levels than α_{669} studied under the same conditions, although as shown in the summary below this was not consistently observed. This indicates much higher activity of $\alpha_{728}\beta\gamma$ at the membrane despite lower cleavage and rules out that trimeric channel activation was due to enhanced expression or processing.

Monomeric α_{728} when injected at 10 fold higher cRNA levels could be observed at the plasma membrane; however, this also

exhibited no evidence of endogenous cleavage. Interestingly, when cleaved as part of trimeric complex, α_{728} was consistently of higher M.W. than that of α_{669} (**Fig. 5B**) indicating the presence of different cleavage location or additional biochemical modification to account for this 4 kDa difference. Alternatively, this differences is consistent with the 26 amino acid fragment between the 2 putative furin cleavage sites, RSRR and RRAR (see Discussion).

Baseline expression and processing and effects of $[Na^+]$ are summarized in **Figure 5C**. Overall both isoforms exhibited much lower membrane than intracellular levels, especially given differences in loading equivalents between these fractions. Full length levels of $\alpha_{728}\beta\gamma$ and $\alpha_{669}\beta\gamma$ were similar in the intracellular fractions irrespective of the $[Na^+]$ ruling out increased protein expression as the explanation for $\alpha_{728}\beta\gamma$ hyperactivity. Membrane full length and cleaved $\alpha_{728}\beta\gamma$ were also lower than those for $\alpha_{669}\beta\gamma$ and this was especially evident in high Na^+. Thus, despite the 18 and 2.5 fold higher activity of $\alpha_{728}\beta\gamma$ in low and high Na^+, there were no comparable increases and in fact lower absolute levels of cleaved α_{728} than α_{669} indicating that the cleaved form is not the only one which supports high activity.

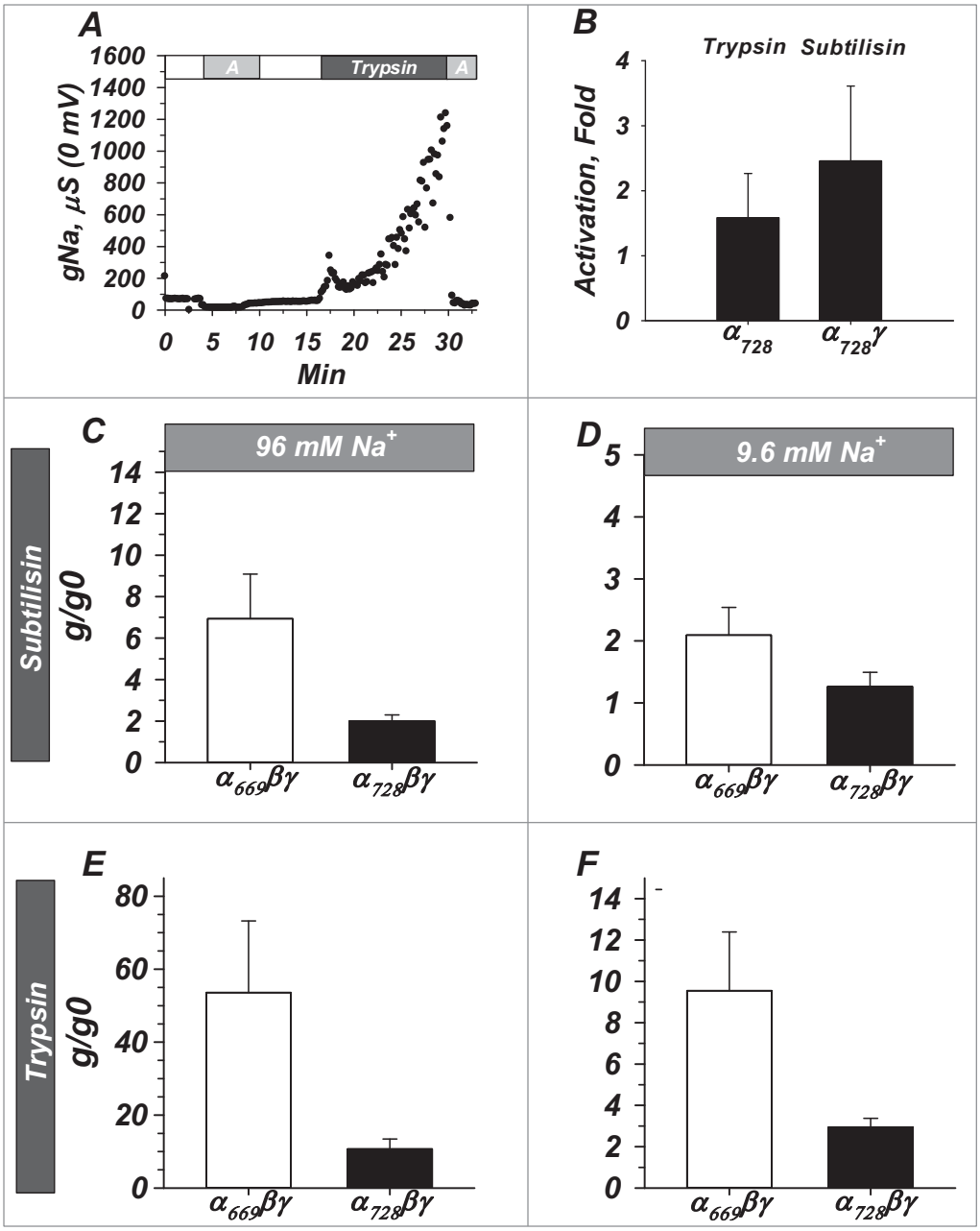

Figure 4. $\alpha_{728}\beta\gamma$ is less sensitive to proteolytic activation than $\alpha_{669}\beta\gamma$ and activation of both isoforms is $[Na^+]$ dependent. (**A**) Example demonstrating similar time course of activation with trypsin to that previously observed with $\alpha_{669}\beta\gamma$ (not shown). "A" indicates 10 μM amiloride. (**B**) Activation required the presence of all 3 subunits similar to that required for α_{669} (not shown) as activity of α_{728} alone and $\alpha_{728}\gamma$ were not appreciably activated by proteases. (**C and D**) Activation by subtilisin and trypsin (**E and F**) in high and low Na^+. In both cases α_{728} was less sensitive to activation by proteases and in both isoforms a larger activation was observed in high Na^+. Note similar profile but difference in scale between subtilisin and trypsin. n = 6-20 for B, 17 for C and D, 14 for E and F. ($P < 0.05$ for all comparisons between isoforms except panel B)

Examination of the proportion of cleaved α at the membrane (**Fig. 6**) indicates similar cleavage proportion between α_{728} and α_{669} despite the lower absolute levels of the cleaved form and the much higher whole cell currents in α_{728}. This indicates that the additional 59 a.a. in α_{728} do not markedly affect overall cleavage efficiency per se, although a shift in cleavage preference cannot be ruled out. This also indicates that the reduced activation of α_{728} trimers with trypsin and subtilisin are likely due to saturation of P_o of existing and likely high activity uncleaved channels.

Also notable in **Figure 6** are the larger cleaved fractions of both isoforms in 96 mM than 9.6 mM Na^+. These differences are opposite to the differences of $[Na^+]$ on activity and are

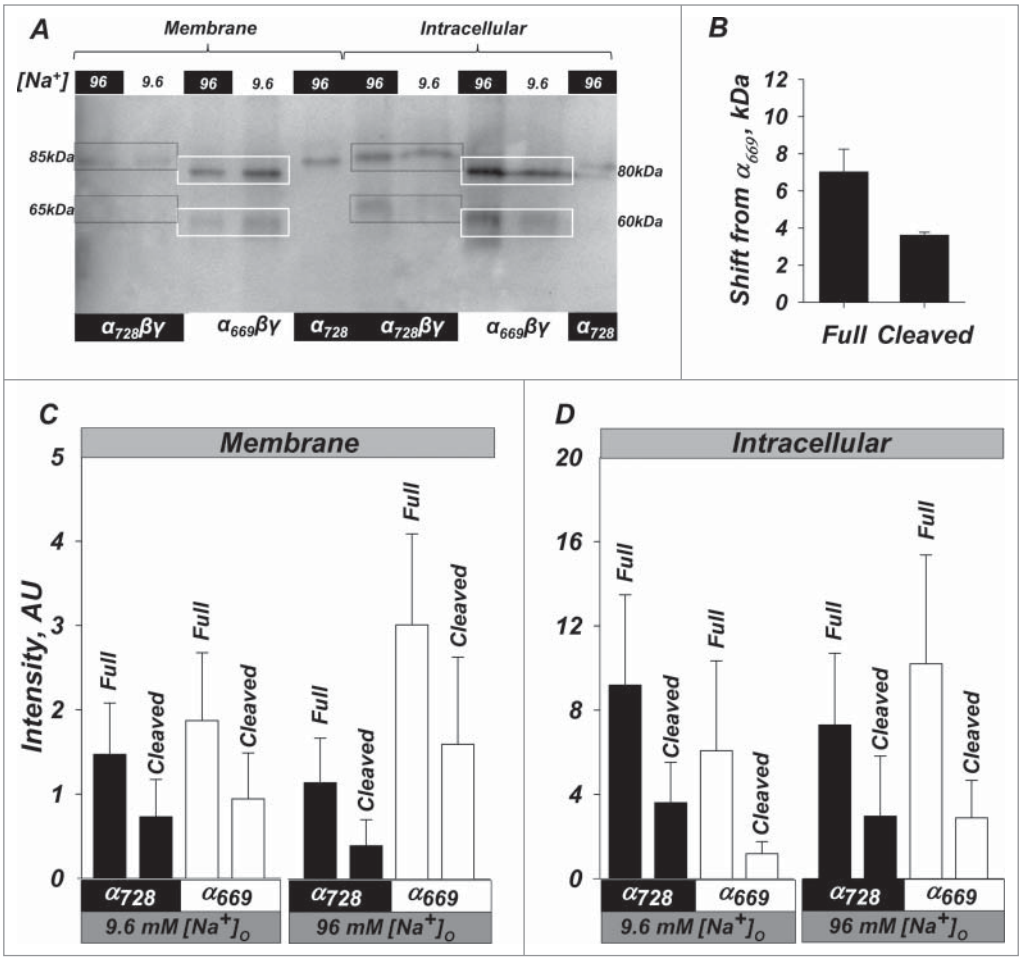

Figure 5. High activity of $\alpha_{728}\beta\gamma$ is not due to increased endogenous processing or membrane density. Western blot of oocytes expressing $\alpha_{669}\beta\gamma$, $\alpha_{728}\beta\gamma$, and α_{728}. (**A**) Representative example showing relative size and intensity of protein as either membrane or intracellular fractions. Membrane and intracellular lanes were loaded with the equivalent yield of 20 and 2 oocytes, respectively. The membrane was probed with an anti-HA antibody. Lower cleavage is observed in the membrane fraction in $\alpha_{728}\beta\gamma$ in low and high Na^+. Higher intracellular cleavage was in general observed in high Na^+. Boxes indicate the size of the full length and large C-terminal fragments and demonstrate an example of the shift in size for full length and cleaved fragments (85 vs 80 and 65 vs 60 kDa). (**B**) Average shift of full length and cleaved forms of α_{728} from that observed for α_{669}. Some differences were retained even in the cleaved subunit indicating possible differences in cleavage site or cleaved subunit modification between the 2 isoforms (see text, $P < 0.05$). (**C**) Summary of the expression at the plasma membrane. α_{728} proteins levels were consistently lower than those of α_{669}. This was markedly evident for both the full length and cleaved fragments in high Na^+ conditions. (**D**) Expression in the intracellular fraction was more robust and no major differences could be observed between the 2 α isoforms in both high and low Na^+. N = 8.

consistent with a different mode of channel regulation by Na^+ that is separate from that by cleavage (see Discussion and **Fig. 12**).

Detection in human urine

Although Thomas et al.[7] detected α_{728} mRNA in human kidneys, the correlation between mRNA concentrations and steady state protein levels is not always strong.[23] Moreover, the *in vivo* cleavage status of this protein was undetermined. As normal human tissue is not readily available for examining protein expression we isolated and examined various urinary fractions for the presence of α_{728} protein. We fractionated urine into organellar and exosomal fractions because exosomes contain plasma membrane bound proteins and this fraction is known to heavily contain aquaporin 2, a membrane protein along with ENaC present in the collecting duct (data not shown).[24]

We examined fractions corresponding to cell debris, large vesicles such as the Golgi apparatus, and exosomes. We used an α_{728} specific antibody. As shown in **Figure 7** we detected full length protein which migrated at 87 kDa consistent with that expected from full length uncleaved α_{728}. A second band at 27 kDa was detected in some subjects which was also competed with the immunizing peptide, and this likely represented the cleaved N-terminal fragment. No C-terminal fragment was detected as the recognized epitope is contained within the first 59 a.a. This indicates the presence of both full length and potentially cleaved α_{728} in human kidneys *in vivo* and also variable cleavage between subjects of this isoform by existing urinary proteases. Additional bands were also detected at less than 20 kDa in some participants (see **Fig. 7**). These fragments may be the products of further proteolytic processing when exosomes are exposed to further urinary proteases.

Cell attached recordings

For both isoforms incubation in high $[Na^+]$ increased the degree of activation by cleavage. Under both Na^+ conditions $\alpha_{728}\beta\gamma$ was also less sensitive to proteolytic activation but displayed higher baseline activity than $\alpha_{669}\beta\gamma$. We used single channel recordings to examine if these differences were due to differences in the single channel conductance or channel kinetics.

Cell attached patch clamp recordings of $\alpha_{728}\beta\gamma$ are shown in **Figure 8**. Under high $[Na^+]$ the single channel conductance was 4.0 pS-similar to the single channel conductance of $\alpha_{669}\beta\gamma$.[25,26] The single channel conductance in low $[Na^+]$ was 1.7 pS. Under both $[Na^+]$ open and close times were consistent with known values for $\alpha_{669}\beta\gamma$. These values are consistent with those of

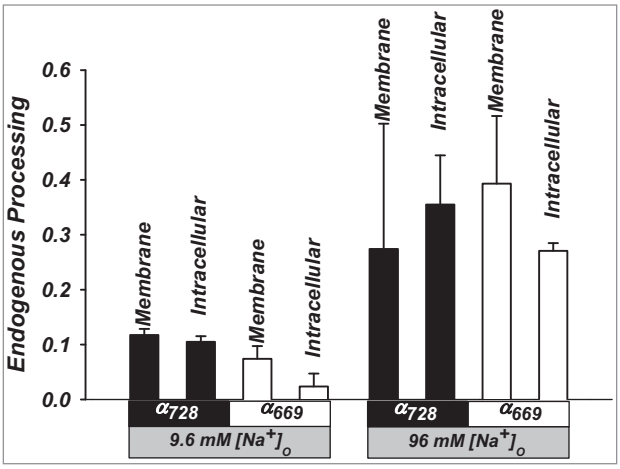

Figure 6. Summary of the proportion of processing of α_{728} and α_{669} in trimeric channels. Data summarized as the ratio of cleaved to full length subunit levels. Similar cleavage proportions are observed for both isoforms in the plasma and intracellular membrane fractions at the same $[Na^+]$. n = 6-8 in all groups. ($P < 0.05$ between high and low Na^+).

Thomas et al. in high Na^+.[7] There were also no marked differences in channel kinetics, however, a direct determination of channel open probability was limited by the slow nature of the ENaC kinetics and variable gating.[27,28] These data along with the Western blot data above rule out that activation of $\alpha_{728}\beta\gamma$ occurs by enhanced membrane density, enhanced single channel conductance, and indicate that activation must be by elimination due to effects on open probability.

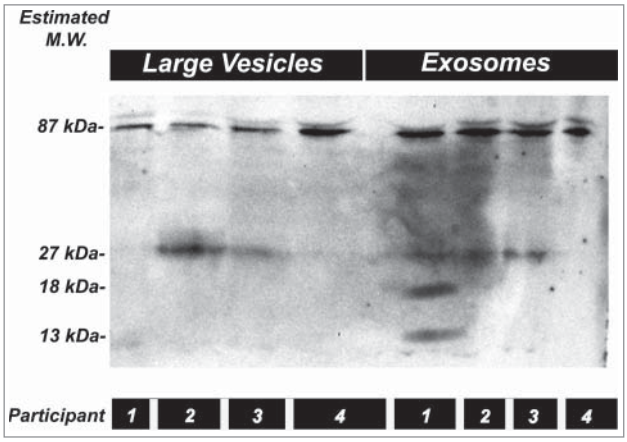

Figure 7. α_{728} protein is present in human kidneys. Two fractions isolated from the urine of 4 subjects representing large vesicles/intracellular organelles, and exosomes. Western blot was probed with an α_{728} specific antibody. The two main bands detected at 87 and 27 kDa, likely correspond to full length and the N-terminal fragment of this isoform. The 27 kDa fragment was not detected in all fractions possibly indicating differences in endogenous cleavage between these individuals. Additional smaller fragments may have originated from further processing by urinary proteases. Data representative of 6 different subjects.

Ideally, single channel measurements would provide evidence of differences in P_o, however, too many channels were observed in all $\alpha_{728}\beta\gamma$ patches and this required that we inject 5 fold less cRNA for the channel subunits, which further precluded an accurate assessment of this parameter. Also, such measurements would fail to show changes of P_o if multiple open states are observed as we propose below in response to cleavage, sodium inhibition and changes of membrane order.

Temperature response

ENaC is activated by low temperature, most likely by increasing open probability following membrane rigidification.[20,21] Given the time course and reversibility, this process represents a cleavage independent means of activating membrane resident channels. We examined the response of $\alpha_{728}\beta\gamma$ channels to a temperature change in the range of 23°C to 10°C.

As shown in **Figure 9**, both isoforms exhibited similar effects of cooling and no significant differences were observed. A decrease from 23°C to 15°C increased the activity of $\alpha_{669}\beta\gamma$ and $\alpha_{728}\beta\gamma$ by 1.3± 0.2 and 1.4± 0.3 fold, respectively. At 10° C, and despite the drop of the single channel conductance [20,21], g_{Na} remained at 1.0± 0.1 and 1.1± 0.3 that observed at 23°C for $\alpha_{669}\beta\gamma$ and $\alpha_{728}\beta\gamma$. This indicates that activation by α_{728} is not due to differences in the way the channel interacts with the membrane and that this mode of activation is unaltered between the 2 isoforms.

Sodium inhibition

We find different effects of prolonged $[Na^+]$ changes on the baseline activity of these 2 α isoforms. Further, differences between the 2 isoforms in terms of rectification and voltage activation indicate variability in the acute effects of $[Na^+]_i$. Given the importance of acute regulation by Na^+, we examined the effects of acute increases of $[Na^+]_i$ by mechanical and electrical forces.

Mechanical loading allowed us to examine the acute effects of changing $[Na^+]_i$ with initial changes occurring within 10s-within the time expected for diffusion from the injecting electrode to the oocyte membrane - and stable concentrations are observed within 2-4 minutes.[14] Experiments were done in 2 groups of oocytes starting in low and high Na^+ baselines. As shown in **Figure 10A** in high Na^+ an increase of $[Na^+]_i$ by 25 mM inhibited $\alpha_{669}\beta\gamma$ by 83% of control, similar to that previously reported.[14] The same increase in $\alpha_{728}\beta\gamma$ caused an initial stimulation to 175% of control followed by inhibition to 42%. Accounting for the initial increase to 175%, similar magnitude of inhibition is observed in both $\alpha_{728}\beta\gamma$ and $\alpha_{669}\beta\gamma$ at the final $[Na^+]_i$ of ~90 mM (175% to 42% vs. 100% to 17%).

The differences in the initial response likely indicate that $\alpha_{728}\beta\gamma$ required that higher $[Na^+]_i$ are achieved prior to inhibition, and that this channel goes through an intermediate concentration near 65 mM where activation of the single channel current by increasing $[Na^+]_i$ dominates leading to a stimulation. This interpretation also requires that $\alpha_{669}\beta\gamma$ single channel current is already saturated at this $[Na^+]_i$ in agreement with measurements of the whole cell conductance (**Fig. 3**).

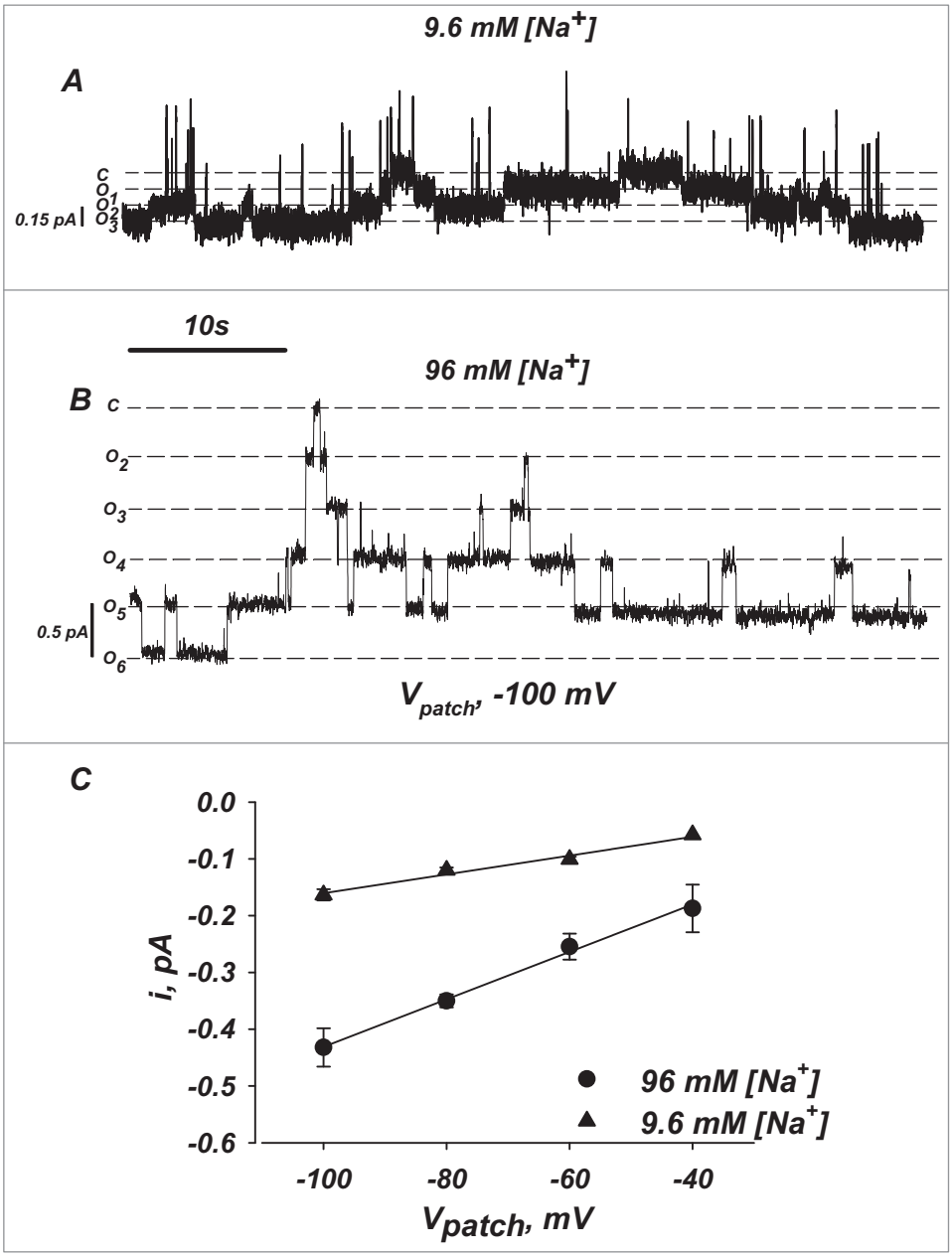

Figure 8. Single channel conductance and open/close times for $\alpha_{728}\beta\gamma$ channels. Single channel recordings were made in cell attached mode. (**A and B**) Representative current traces of $\alpha_{728}\beta\gamma$ at −100 mV under low and high $[Na^+]$. (**C**) Single channel I/V relationship of $\alpha_{728}\beta\gamma$ in low and high $[Na^+]$. Both conductance and kinetics were similar to those observed for $\alpha_{669}\beta\gamma$ (not shown, see Thomas et al.[7]). Oocytes were injected with 5 fold less cRNA to allow channel recordings in stable patches. n = 4.

A 25 mM increase of $[Na^+]_i$ from a low baseline of 12 mM is shown in **Figure 10B**. In both cases the final conductance obtained in 37 mM $[Na^+]_i$ was stimulated to the range of 132-142% of control. However, the initial responses obtained as $[Na^+]_i$ increased from 12 to 37 mM were markedly different between the 2 isoforms indicating likely differences in the increase of single channel current by Na^+. In the case of $\alpha_{728}\beta\gamma$ it exhibited an initial increase to 175% of control, while $\alpha_{669}\beta\gamma$ exhibited a larger increase to 380% of control. As the $[Na^+]_i$ stabilized, $\alpha_{728}\beta\gamma$ exhibited little further effects while $\alpha_{728}\beta\gamma$ was inhibited nearly 3 fold (from 380% to 140%). These effects complement the changes observed in panel A and together indicate that the acute Na^+ sensitivity of $\alpha_{728}\beta\gamma$ is shifted to the right of that of $\alpha_{669}\beta\gamma$ where both the initial increase and subsequent inhibition occur at higher $[Na^+]_i$.

To examine the acute effects of variable and incremental increases of $[Na^+]_i$ we voltage clamped membranes to −100 mV. Shown in **Figure 11A** are the effects of a voltage driven Na^+ loading from a high baseline of 70 mM $[Na^+]_i$. Similar to the results of **Figure 10**, a larger initial increase is observed in $\alpha_{728}\beta\gamma$. This was smaller in magnitude to that observed above given that the changes here are more gradual. Similarly, a larger final inhibition is observed in $\alpha_{728}\beta\gamma$ but at a higher $[Na^+]_i$ consistent with the interpretation above that $\alpha_{728}\beta\gamma$ is rightward shifted in terms of sodium sensitivity.

Voltage loading from a low $[Na^+]_i$ of 12 mM is shown in **Figure 11B**. Consistent with the data above a small stimulation followed by inhibition is observed for $\alpha_{669}\beta\gamma$ as $[Na^+]_i$ increased past 20 mM. Given the high conductances of $\alpha_{728}\beta\gamma$ oocytes, and consistent with the expectation from **Figure 10** that clamping to −100 mV would result in further marked stimulation of the conductance in low Na^+, currents produced in this group were both too large to reliably clamp and damaging to the oocytes. For these reasons these experiments could not be carried out.

Discussion

$\alpha_{728}\beta\gamma$ forms a highly active channel

We report that the longer N-terminus in α ENaC modifies channel properties and regulation. Our data show that $\alpha_{728}\beta\gamma$ channels showed differences in rectification and voltage activation; both intrinsic channel properties. Additionally, $\alpha_{728}\beta\gamma$ channels are highly active despite similar single channel conductance to $\alpha_{669}\beta\gamma$ and lower density at the membrane than $\alpha_{669}\beta\gamma$. This was observed in spite of little response to activation by proteolysis and notwithstanding the low levels of endogenous cleavage of α_{728} at the membrane. This isoform also responded differently to both chronic and acute changes in $[Na^+]$ indicating a rightward shift in the sensitivity to changes of $[Na^+]_i$. Despite these

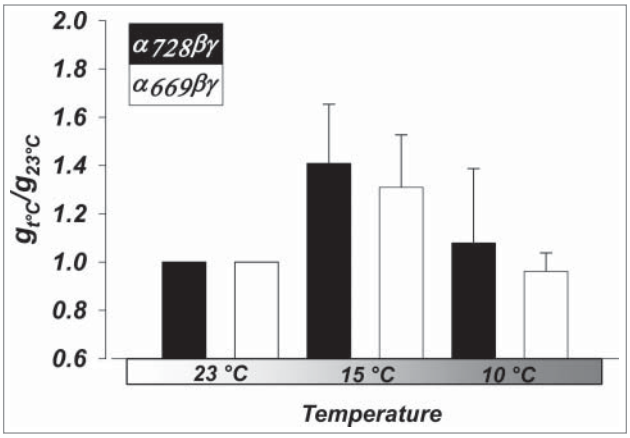

Figure 9. Activation of αβγ ENaC by cooling is similar, regardless of α isoform. Changes in whole-cell amiloride-sensitive conductance at 15°C, and 10°C were normalized to conductance at 23°C. n = 6. ($P < 0.05$ between all temperatures, but NS between isoforms).

marked differences, $\alpha_{728}\beta\gamma$ was activated by cold temperature similar to $\alpha_{669}\beta\gamma$. Thus, based on the relative expression of short vs. long α we expect major changes to epithelial sodium handling and intrinsic regulation in humans.

As α_{728} is present in the kidney it is reasonable to conclude that this isoform serves a biological function that is distinct from that of α_{669}. A high activity form of ENaC may have a desired role in preventing either salt wasting, or hyponatremia and an undesired role of promoting salt sensitive hypertension. This isoform could have developed evolutionarily as means of conserving sodium in a rare sodium environment.

A variety of lines of evidence point to α_{728} behaving more like αrENaC than α_{669} hENaC. It has higher baseline activity, as well as homology to the rat sequence. Consistent with this explanation is the lower activation of rodent ENaC by trypsin than that observed in the short human isoform.[16,29]

$\alpha_{728}\beta\gamma$ fragments and processing

Full length α_{728} migrated at a size consistent with the presence of an additional 59 a.a. to α_{669}. However, cleaved α_{728} was 4 kDa larger than cleaved α_{669}. Currently, 2 sites have been have been proposed and validated to be cleaved by endogenous furin type proteases.[29] These sites are approximately 26 a.a. apart. This shift in mass would be consistent with a shift in preference of cleavage between α_{669} and α_{728} from the second furin site (RRAR) to the first furin site (RSRR) resulting in a large cleaved fragment in α_{728} which is 26 a.a. longer. Alternatively, one would have to propose post translational differences between the 2 subunits occurring prior to cleavage; as cleavage in the same location in the absence of either explanation would result in an identical product for the 2 α isoforms. This remains to be tested but would allow toggling between regulatory pathways affecting each isoform independently.

Cleavage of α_{728} in urinary exosomes was variable between subjects. Invariably, the full length isoform was observed at 87 kDa. A product at 27 kDa was observed (see **Fig.** 7 and supplementary Figure). The intensity of this product was variable demonstrating possible variability among subjects. The size of this product is consistent with cleavage at the first furin site; although we cannot rule out additional processing of these fragments by the urinary

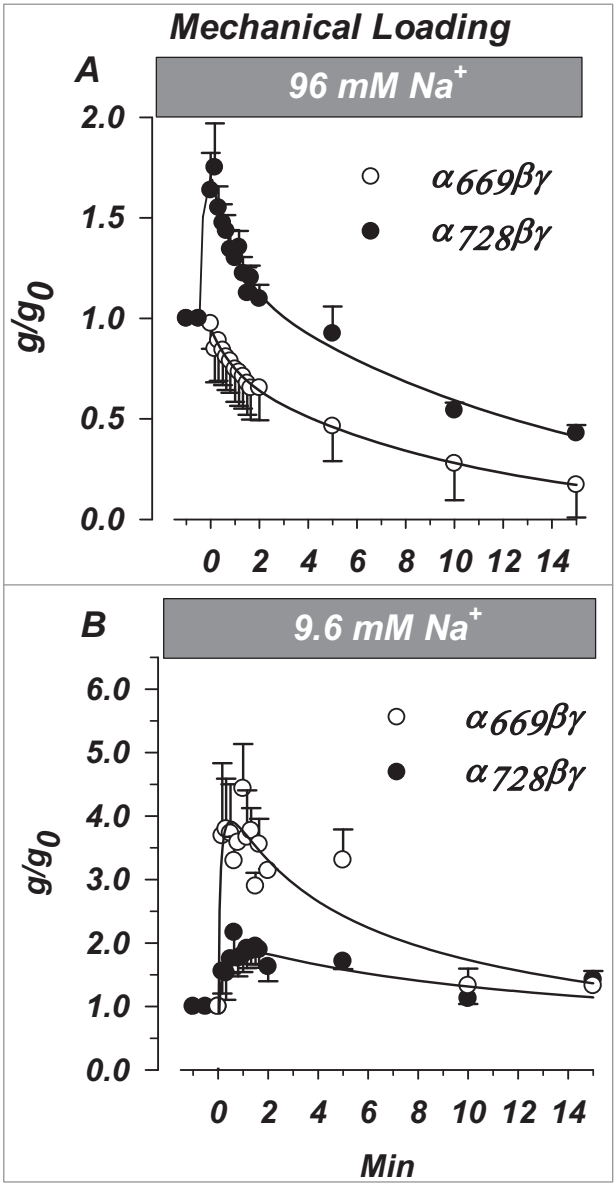

Figure 10. Changes of ENaC activity by acute increases of $[Na^+]_i$ is isoform dependent. Oocytes were injected with 25 mM Na^+ as described in text. Amiloride sensitive conductance was recorded at −100 mV and normalized to that immediately before Na^+ injection. (**A**) Changes in $\alpha_{669}\beta\gamma$ or $\alpha_{728}\beta\gamma$ expressing oocytes studied in high $[Na^+]$ in response to an increase of $[Na^+]_i$ from 65 to 90 mM. (**B**) Changes in $\alpha_{669}\beta\gamma$ or $\alpha_{728}\beta\gamma$ expressing oocytes studied in low $[Na^+]$ in response to an increase of $[Na^+]_i$ from 12 to 37 mM. The two α isoforms displayed marked differences indicating higher sensitivity of α_{669} to changes of $[Na^+]_i$ from a low baseline. Together these data indicate that inhibition of α_{728} by increasing Na^+ occurs at $[Na^+]_i > 37$ mM making this isoform different in the way it responds to Na^+ than α_{669}. (n = 6 in each group). $P < 0.05$ for the time dependent differences between the 2 isoforms except the ending points (last 2) in (B).

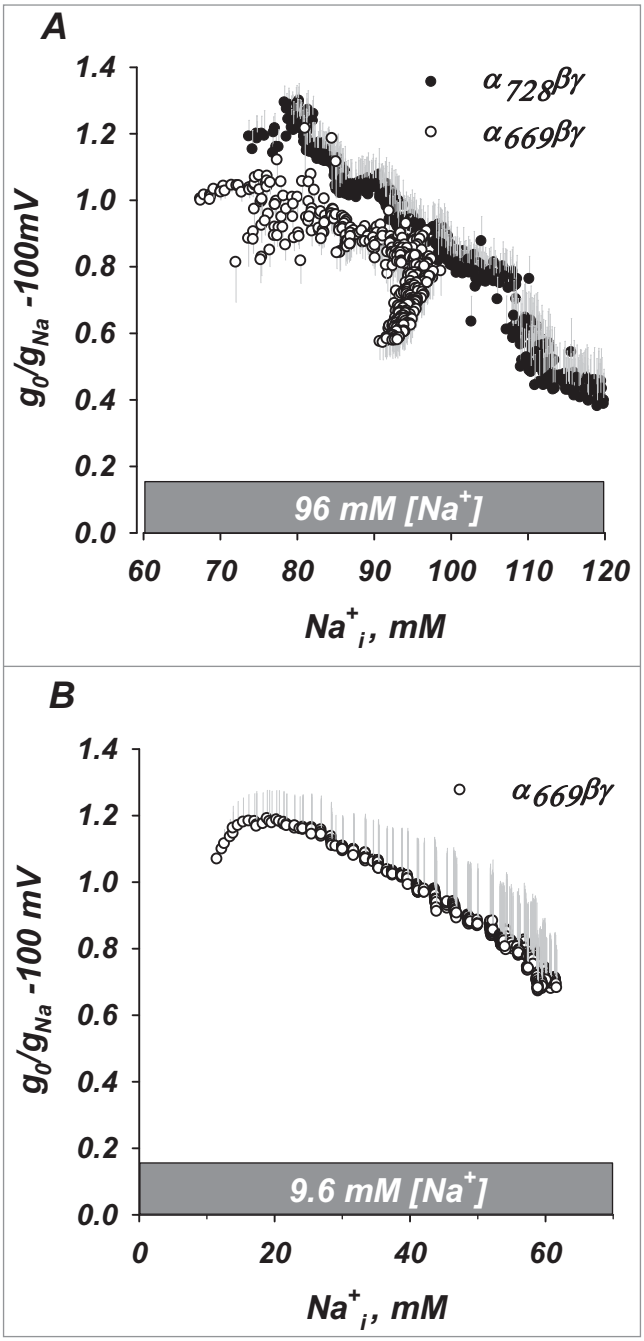

Figure 11. Inhibition of ENaC by acute voltage induced increases of $[Na^+]_i$. (**A**) Inhibition of both isoforms from a baseline $[Na^+]_i$ of 65 mM. (**B**) Inhibition at low $[Na^+]_i$ baseline could only be measured in $\alpha_{669}\beta\gamma$ due to the high expression of $\alpha_{728}\beta\gamma$. (See text.) In these experiments similar inhibition of $\alpha_{669}\beta\gamma$ was observed to that with mechanical loading in **Fig. 10B**. n = 4.

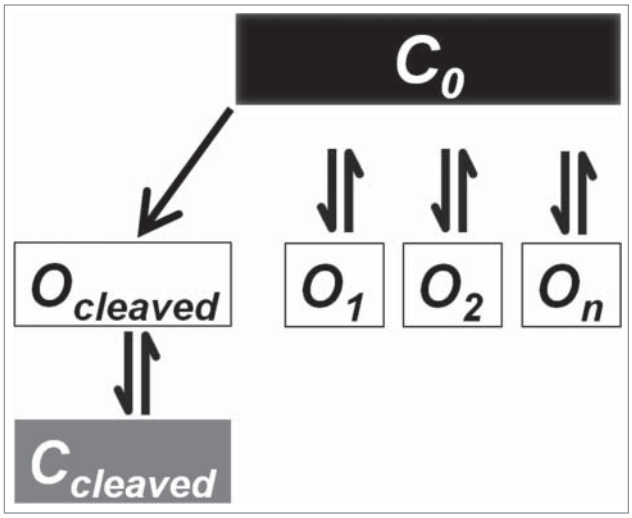

Figure 12. Proposed multiple open state model for ENaC to describe the separate effects of cleavage, sodium concentration and temperature. In this model we propose that there is a single closed state "C_0," and multiple non-interacting open states "$O_1 \ldots O_n$." This model explains how some means of increasing P_o are unchanged between isoforms (such as temperature), while others (such as activation by proteases) show distinct differences. It also accounts for the high baseline activity in low Na^+ under conditions with little cleavage. See Discussion for details.

proteases as evident by the presence of additional smaller fragments that were competed with excess immunizing peptide.

Protease activation in high and low Na^+

The fraction of cleaved to full length protein expression was similar for trimeric channels expressing α_{728} or α_{669}. This indicates that the extended N-terminus does not hinder access of endogenous proteases to the channel. However, there were marked differences in the response of these channels to exogenous proteases in a manner that is $[Na^+]$ dependent. Moreover, there are also differences in the levels of baseline cleavage of these isoforms in different $[Na^+]$.

Proteolytic activation provides a mechanism for rapid channel activation and is therefore an important acute regulator of Na^+ absorption especially given the abundance of urinary proteases which could potentially act on ENaC.[30,31] Our data show that the ratio of channel activation by cleavage (**Fig. 4**), and also baseline cleavage (**Fig. 6C**), are positively correlated with the $[Na^+]$. We also show that the activity of trimeric α_{728} is negatively correlated with cleavage and $[Na^+]_i$ (**Figs. 3 and 6**). The similarity in profile of cleavage by trypsin, subtilisin and endogenous proteases indicate that the differences in $[Na^+]$-dependent activation are generalized effects. This has been interpreted by others as a relief of Na^+-self inhibition by cleavage.[32] However, when comparing α_{728} to α_{669} at high Na^+ such an interpretation would be inconsistent with the larger effects of increasing $[Na^+]_i$ on $\alpha_{728}\beta\gamma$ (**Fig. 10A**), and the lower stimulation by exogenous cleavage of this isoform (**Fig. 4C and E**). Irrespective of the exact mechanism, this effect of $[Na^+]_i$ on cleavage could represent a valuable mechanism to preserve pools of uncleaved channels to respond to recoveries from periods of elevated sodium conditions.

We find that both α isoforms are most active under low $[Na^+]$; the condition which exhibits the least endogenous proteolysis and the least fold activation by external proteases. Therefore, the high baseline activity seen under low $[Na^+]$ and that seen through proteolytic activation at high $[Na^+]$ cannot occur

through the same mechanism. Thus, more than one channel open state must exist to account for these 2 processes. We denote these 2 open states as $O_{cleaved}$ and O_1 (summarized below).

The exact ratio of different α isoforms in the collecting duct, or other human epithelia for that matter, is unknown. However, it is known that activation by proteases in native and even cultured epithelial tissue is variable.[33] Such variability may possibly reflect different $[Na^+]_i$ conditions and also multiple channel pools with differing activity due to different α subunit composition.

Na^+ sensitivity

The driving forces across the apical membrane and by extension $[Na^+]_i$ in an epithelium is, unlike that in a single non-polarized cell, dependent on numerous factors that include apical and basolateral permeability as well as paracellular shunt resistance.[34] We examined the responses of both α isoforms in the concentration range of 12-110 mM $[Na^+]_i$. Given a Na^+ activity coefficient in the range of 0.8 [35] these represent activities in the range of 9.5–88 mM. The upper end of activity does not necessarily represent physiological values however, the entire scale is broad and covers low baseline values normally encountered [36-39], higher values that are or could be encountered, and high values that aid in better describing the complete relationship and differences in the effects of $[Na^+]$ on $\alpha_{728}\beta\gamma$. The ease of manipulating these concentrations represents an important strength of the oocyte system.

Our data indicate clear differences in the response of these 2 isoforms to Na^+ throughout the entire range of activities examined. Channels formed with α_{728} exhibited a rightward shift in the response to $[Na^+]_i$. In other words, they were less sensitive to inhibition by Na^+ than α_{669}. In the range of activities which could be encountered in the collecting duct of 28 mM or less[39], α_{728} channels exhibited further activation by increasing $[Na^+]_i$ and this occurred in a cleavage independent manner. A simple hypothesis that could explain this effect is that the extended N-terminus in α_{728} may contain or modify a Na^+ sensor. The latter explanation is more feasible as the former would require the presence of multiple Na^+ sensors and high and low sensitivity to inhibition of α_{728} by Na^+.

Irrespective of the biophysical basis, alternative responses to $[Na^+]$ between isoforms may provide tissue specific responses to $[Na^+]$. For example, in the kidney it may be desirable to have a rapid decrease in absorption in response to an acute increase in luminal $[Na^+]$ to buffer against transient changes in $[Na^+]$ changing blood volume; while in the lung it may be desirable to have a slower response to acute changes in plasma $[Na^+]$ to prevent edema. These differences are further highlighted if one considers possible differences in $[Na^+]_i$ between different epithelia.

Kinetic model

Activations of ENaC by cold and by proteolysis likely represent distinct processes that increase open probability. Activation by cold is reversible, while that by cleavage is irreversible. Cold activation occurs through rigidification of the membrane, while proteolytic activation occurs through either loss of the first transmembrane domain,[19] or loss of an inhibitory peptide.[18] Our data further highlight and confirm these differences as proteolytic activation for these two isoforms was markedly different but temperature dependent activation was the same. This indicates that these two open states cannot be the same and further cannot communicate otherwise temperature activation of $\alpha_{728}\beta\gamma$ would be different than $\alpha_{669}\beta\gamma$. These two modes of activation are likely due to two different non-communicating open states rather than closed non-communicating states, although the latter cannot be excluded. These are denoted as $O_{cleaved}$ and O_2.

Our data also indicate that a large part of $\alpha_{728}\beta\gamma$ baseline activity could occur in the absence of cleavage. This requires the presence of a third distinct open state. This state was described above and denoted as O_1. It is also likely non-communicating with other open states as $\alpha_{728}\beta\gamma$ is still subject to similar activation by cold. This state is also observed in $\alpha_{669}\beta\gamma$ given its high activity in the absence of appreciable endogenous cleavage in low $[Na^+]$. This multiple open state model is illustrated in **Figure 12**. For simplicity, only multiple open states are illustrated, although the data are also explained by multiple non-communicating closed states.

This model offers a kinetic explanation for the low sensitivity to proteolysis in $\alpha_{728}\beta\gamma$ as well as $\alpha_{669}\beta\gamma$ in low $[Na^+]$: the proteolytic substrate may only become accessible to digest in a closed state. High activity in low $[Na^+]$ (or in general for $\alpha_{728}\beta\gamma$) would cause a higher occupancy of the open state, and reduced sensitivity to cleavage. Additional tests for these predictions are required; however, the similarities and difference between $\alpha_{728}\beta\gamma$ and $\alpha_{669}\beta\gamma$ activation by cleavage, cold temperature and baseline activity provide clear evidence for supporting the presence of multiple states.

Modularity of ENaC

In addition to δ, and α_{669}, α_{728} is a third human ENaC subunit that can form distinct high activity channels with β and γ. Several examples exist of ion channels with subunit modularity either due to alternative splicing or alternate subunits, including voltage gated calcium channels,[40,41] and voltage gated potassium channels.[42] The modularity of ENaC may also explain some of the interpersonal or inter-population differences in Na^+ handling and blood pressure. The ENaC sequences themselves are highly conserved, but differential expression of alternatively spliced α or expression of δ may account for individual or population level variations in both activity and regulation of activity.

Materials and Methods

RNA

The extra 177 bases from the longer α isoform were synthesized (Genscript, Piscataway NJ) (NCBI accession # NM_001159576) and ligated upstream of the start site into a DNA plasmid containing the coding sequence for α_{669} which also contained 2 HA tags as previously described.[43] This plasmid was linearized and translated into RNA with the RiboMAX T7 transcription kit (Promega, Madison WI). Capped RNA was

quantified with a Nanodrop 1000 spectrophotometer (ThermoFisher, Waltham MA), and by RNA gel electrophoresis. This assured equal injection of all ENaC subunit isoform cRNAs.

Xenopus oocytes

Xenopus (Xenopus Express, Brooksville FL) oocytes were obtained by surgical excision of the ovarian lobes. Oocytes were digested with type IA collagenase (Sigma-Aldrich, St. Louis MO) in Ca^{2+} free OR2 medium as previously described.[44] Stage V and VI oocytes were selected and allowed to recover overnight in ND94 medium with (94 mM NaCl, 1 mM $MgCl_2$, 1.8 mM $CaCl_2$, 2 mM KCl, 5 mM HEPES, pH 7.4) containing 1% penicillin-streptomycin (Mediatech, Corning NY) and 50 μg/ml amikacin (MP Biomedical, Solon OH).

Oocytes were injected with 2.5 ng RNA for each ENaC subunit, except those which expressed α alone which were injected with 25 ng. Oocytes were then incubated in the 96 mM Na^+ incubation solution (chronic high Na^+) or a similar solution that contained 9.6 mM NaCl and replaced the rest with 86.4 mM N-methyl-D-glucamine (chronic low Na^+). Oocytes were recorded from 18-72 hours post injection. Western blot analyses were performed on protein homogenates obtained from oocytes 48–72 hours post injection.

Two electrode voltage clamp

Oocyte recordings and calculation of membrane conductance and capacitance were carried out as previously described.[22] Briefly, oocytes were clamped to a holding potential of either 0, or −100 mV with a TEV-200 voltage clamp (Dagan Instruments, Minneapolis MN). Conductance and capacitance were measured every 10s as the slope conductance at the holding potential. In these experiments current/voltage relationships were measured by 500 mS pulses from −100 to +40 mV. Clamping was carried out using agar-Ag/AgCl electrodes as previously described to avoid flow and time dependent artifacts.[45]

In experiments which acutely Na^+ loaded oocytes, or following intracellular Na^+ injection, voltage was clamped to −100 mV (see Mechanical Loading). In both cases, and unless otherwise noted, all reported values of conductance represent the amiloride sensitive portion (10 μM amiloride). In all experiments the recording chamber was continuously perfused at 8 mL/minute.

Mechanical loading (Sodium Injection)

Oocytes were clamped to 0 mV and injected with a 27.6 nL bolus of 0.5 M Na_2SO_4 to increase $[Na^+]_i$ by 25 mM as previously described.[14] Na_2SO_4 was selected to avoid any effects of chloride. To sustain high $[Na^+]$ and prevent efflux of injected Na^+, injected oocytes were clamped to −100 mV for the 1st 2 min, followed by a return to 0 mV to prevent large increases in $[Na^+]_i$. The slope conductance at −100 mV was measured by a 500 ms pulse protocol.

Voltage loading (−100 mV clamp)

Oocytes were acutely loaded with Na^+ by clamping to −100 mV for up to 20 min. This allowed larger and more variable changes of $[Na^+]_i$. In these experiments, slope conductance at −100 mV and reversal potential were measured every second by applying a voltage ramp from −100 mV to +20 mV for 100 ms; with membrane voltage remaining clamped to −100 mV for the remaining 900 ms. Input and output signals were generated or recorded at 5 kHz yielding a voltage change during the ramp of 0.24 mV per point. The command voltage signal was generated, and the current return signal was measured by a National Instruments MyDaq data acquisition board (Austin TX), captured in NI Signal Express, and analyzed in R (R Project for Statistical Computing). This protocol allowed us to clamp membrane potential to −100 mV 90% of the time and to examine the effects of internal $[Na^+]$ on inhibition with high time resolution.

Cell attached patch clamp

Oocytes were devitellinized by shrinking for 5 min in 100 mM sucrose in high or low $[Na^+]$ solutions, followed by manual removal of the vitelline membrane. Oocytes were then allowed to recover in a bath solution of high or low sodium for 10–15 min. The pipette solution matched the bath solution in all cases. Cell attached single channel recordings were carried out at various holding voltages ranging between −100 mV to 0 mV using an Axopatch 200B amplifier (Molecular Devices, Sunnyvale CA) in cell-attached mode with a sintered Ag/AgCl pellet as reference. Signals from seals > 20GΩ were amplified at 500× gain and filtered at 200 Hz. Pipettes with resistances of 1–5 MΩ were pulled from acetone washed Corning 8161 glass (Corning Inc., Corning NY) using a multiple stage horizontal puller (Sutter Instruments, Novato CA). Electrodes were fire polished and tips were coated with polystyrene q-dope (GC electronics, Rockford IL). Signals were digitized at 1 kHz with an ADC (Digidata 1322A, Molecular Devices) and analyzed using Clampfit 9 (Molecular Devices).

Western blot – *xenopus* oocytes

Groups of 50 oocytes were biotinylated for 40 min on a random orbit shaker at 4°C with EZ-Link Sulfo-NHS-SS-Biotin (Pierce, Rockford, IL) at 0.8 mg/ml in ND94. Oocytes were washed 5× and resuspended in 10 μl/oocyte in homogenization buffer containing (150 mM NaCl, 10 mM Tris, 5 mM EDTA, 1% Triton ×-100, pH 7.4). The HB also contained protease inhibitors (Halt Protease Inhibitor Cocktail, Pierce). Oocytes were disrupted with a 25 gauge needle followed by a low speed spin (800 g) at 4°C to remove the yolk. The membrane fraction was pelleted at 18,000 g, resuspended in 10 μl/oocyte in HB, homogenized in a ground glass homogenizer and followed by sonication. The now soluble total membrane fraction was isolated at 18,000 g and used for Western blotting or incubated with Streptavidin conjugated agarose beads (Pierce) for isolation of the plasma membrane fraction. Biotinylated membrane proteins were eluted from the beads for 20 min at 65°C in buffer containing 1% BME. The protein equivalents of 20 or 2 oocytes (for membrane and intracellular, respectively) were loaded per lane on a 7.5% polyacrylamide gel, separated, transferred to nitrocellulose membrane, blocked in 5% milk (TBS-T, (0.05%

Tween-20). Membranes were probed with an anti-HA HRP-conjugated antibody (clone 3F10, Roche Inc., Indianapolis IN) and proteins were visualized by Enhanced Chemiluminescence (Super Signal Dura West, Pierce) in a gel documentation system (MP4000, BioRad Hercules CA). Intensities of raw unadjusted images were analyzed with included imaging software (BioRad).

Western blot – human urine

Urine from 6 participants (50 ml, 3 male and 3 female aged 23 to 70) was sequentially centrifuged at 300 g, 17,000 g and 200,000 g to pellet fractions corresponding to cell debris, intracellular organelles/large membranes, and exosomes, respectively as previously described.[46] The pellet from each centrifugation step was homogenized, treated in 1x Laemmli's reducing buffer for 10 minutes at 37°C. The equivalent protein yield of 3 ml of urine was separated on 10% SDS-PAGE. Proteins were transferred to nitrocellulose membranes, then blocked in 5% milk for 1 h at room temperature, and followed by overnight at 4°C incubation with the primary α_{728} N-terminus specific antibody at a dilution of 1:2000. Membranes were washed 5× and incubated at room temperature with 1:20,000 dilution of the appropriate secondary antibody and visualized as above.

Antibody against α_{728}

An antibody was produced using the peptide sequence "EGTQGPELSLDPDPC," which is unique in humans to the α_{728} N-terminus as an antigen. The rabbit antibody exhibited a titer of >1:200,000 and was antigen purified. Antigenicity was also confirmed by the ability of this antibody to recognize HA-tagged α_{728} and the ability of the immunizing antigen to compete this signal (see **Fig. S1** for further characterization).

Temperature Control

Chamber temperature was controlled by a Dagan HCC-100A temperature controller (Dagan Instruments) and an HE-200 thermal stage modified with an insulating layer of neoprene. Temperature was sampled in the bath and used as feedback for the controller. Chamber inflow was routed in the thermal stage block multiple times to allow pre-equilibration of solution and eliminate temperature variations from the perfusate.

Protease

ENaC expressing oocytes were treated with the serine proteases subtilisin or trypsin (50 ng/ml) for 15 min. The ratio of amiloride sensitive conductance before and after protease treatment was used as the degree of activation.

Significance was determined by Student's t-test. P of <0.05 was deemed significant and levels were indicated by * and ** for $P < 0.05$ and 0.01, respectively. Summarized data are shown as means and standard error of the mean.

Disclosure of Potential Conflicts of Interest

No potential conflicts of interest were disclosed.

Funding

This work was supported by NIH grant DK55626, and by the John R. Oishei Foundation.

Supplemental Material

Supplemental data for this article can be accessed on the publisher's website.

References

1. Anantharam A, Palmer LG. Determination of epithelial Na^+ channel subunit stoichiometry from single-channel conductances. J Gen Physiol [Internet] 2007 [cited 2014 Feb 20]; 130:55-70. Available from: http://www.pubmedcentral.nih.gov/articlerender.fcgi?artid=2154365&tool=pmcentrez&rendertype=abstract; PMID:17562820; http://dx.doi.org/10.1085/jgp.200609716
2. Jasti J, Furukawa H, Gonzales EB, Gouaux E. Structure of acid-sensing ion channel 1 at 1.9 A resolution and low pH. Nature [Internet] 2007 [cited 2014 Feb 21]; 449:316-23. Available from: http://www.ncbi.nlm.nih.gov/pubmed/17882215; PMID:17882215; http://dx.doi.org/10.1038/nature06163
3. Gonzales EB, Kawate T, Gouaux E. Pore architecture and ion sites in acid-sensing ion channels and P2X receptors. Nature [Internet] 2009 [cited 2014 Jan 20]; 460:599-604. Available from: http://www.pubmedcentral.nih.gov/articlerender.fcgi?artid=2845979&tool=pmcentrez&rendertype=abstract; PMID:19641589; http://dx.doi.org/10.1038/nature08218
4. Channel ES, Snyder PM, Mcdonald J, Stokes JB, Welshn MJ. Membrane topology of the amiloride-sensitive. J Biol Chem 1994; 269:24379-83.
5. Babini E, Geisler H-S, Siba M, Gründer S. A new subunit of the epithelial Na^+ channel identifies regions involved in Na^+ self-inhibition. J Biol Chem [Internet] 2003 [cited 2014 Feb 21]; 278:28418-26. Available from: http://www.ncbi.nlm.nih.gov/pubmed/12764146; PMID:12764146; http://dx.doi.org/10.1074/jbc.M301315200
6. Kapoor N, Lee W, Clark E, Bartoszewski R, McNicholas CM, Latham CB, Bebok Z, Parpura V, Fuller CM, Palmer CA, et al. Interaction of ASIC1 and ENaC subunits in human glioma cells and rat astrocytes. Am J Physiol Cell Physiol [Internet] 2011 [cited 2014 Jul 14]; 300:C1246-59. Available from: http://www.pubmedcentral.nih.gov/articlerender.fcgi?artid=3118626&tool=pmcentrez&rendertype=abstract; PMID:21346156; http://dx.doi.org/10.1152/ajpcell.00199.2010
7. Thomas CP, Auerbach S, Stokes JB, Volk KA. 5' heterogeneity in epithelial sodium channel alpha-subunit mRNA leads to distinct NH2-terminal variant proteins. Am J Physiol [Internet] 1998 [cited 2014 Mar 13]; 274:C1312-23. Available from: http://www.ncbi.nlm.nih.gov/pubmed/9612219; PMID:9612219
8. Butterworth MB. Regulation of the epithelial sodium channel (ENaC) by membrane trafficking. Biochim Biophys Acta [Internet] 2010 [cited 2014 Jul 23]; 1802:1166-77. Available from: http://www.pubmedcentral.nih.gov/articlerender.fcgi?artid=2921481&tool=pmcentrez&rendertype=abstract; PMID:20347969; http://dx.doi.org/10.1016/j.bbadis.2010.03.010
9. Chraïbi A, Vallet V, Firsov D, Hess SK, Horisberger JD. Protease modulation of the activity of the epithelial sodium channel expressed in Xenopus oocytes. J Gen Physiol [Internet] 1998 [cited 2014 Feb 27]; 111:127-38. Available from: http://www.pubmedcentral.nih.gov/articlerender.fcgi?artid=1887769&tool=pmcentrez&rendertype=abstract; PMID:9417140; http://dx.doi.org/10.1085/jgp.111.1.127
10. Abriel H, Horisberger JD. Feedback inhibition of rat amiloride-sensitive epithelial sodium channels expressed in Xenopus laevis oocytes. J Physiol [Internet] 1999 [cited 2014 Feb 26]; 516(Ptt 1):31-43. Available from: http://www.pubmedcentral.nih.gov/articlerender.fcgi?artid=2269211&tool=pmcentrez&rendertype=abstract; PMID:10066920; http://dx.doi.org/10.1111/j.1469-7793.1999.031aa.x
11. Chraïbi A, Horisberger J-D. Na self inhibition of human epithelial Na channel: temperature dependence and effect of extracellular proteases. J Gen Physiol [Internet] 2002 [cited 2014 Jul 23]; 120:133-45. Available from: http://www.pubmedcentral.nih.gov/articlerender.fcgi?artid=2234458&tool=pmcentrez&rendertype=abstract; PMID:12149276
12. Anantharam A, Tian Y, Palmer LG. Open probability of the epithelial sodium channel is regulated by intracellular sodium. J Physiol [Internet] 2006 [cited 2014 Feb 26]; 574:333-47. Available from: http://www.pubmedcentral.nih.gov/articlerender.fcgi?artid=1817776&tool=pmcentrez&rendertype=abstract; PMID:16690707; http://dx.doi.org/10.1113/jphysiol.2006.109173
13. Lindemann B. Fluctuation analysis of sodium channels in epithelia. Annu Rev Physiol [Internet] 1984 [cited 2014 Feb 26]; 46:497-515. Available from: http://www.ncbi.nlm.nih.gov/pubmed/6324660; PMID:6324660; http://dx.doi.org/10.1146/annurev.ph.46.030184.002433
14. Awayda MS. Regulation of the epithelial Na(+) channel by intracellular Na(+). Am J Physiol [Internet] 1999 [cited 2014 Feb 27]; 277:C216-24. Available from: http://www.ncbi.nlm.nih.gov/pubmed/10444397; PMID:10444397
15. Awayda MS, Platzer JD, Reger RL, Bengrine A. Role of PKCalpha in feedback regulation of Na(+) transport in

an electrically tight epithelium. Am J Physiol Cell Physiol [Internet] 2002 [cited 2014 Jul 14]; 283:C1122-32. Available from: http://www.ncbi.nlm.nih.gov/pubmed/12225976; PMID:12225976; http://dx.doi.org/10.1152/ajpcell.00142.2002

16. Caldwell RA, Boucher RC, Stutts MJ. Serine protease activation of near-silent epithelial Na^+ channels. Am J Physiol Cell Physiol [Internet] 2004 [cited 2014 Feb 26]; 286:C190-4. Available from: http://www.ncbi.nlm.nih.gov/pubmed/12967915; PMID:12967915; http://dx.doi.org/10.1152/ajpcell.00342.2003
17. Vallet V, Chraibi A, Gaeggeler HP, Horisberger JD, Rossier BC. An epithelial serine protease activates the amiloride-sensitive sodium channel. Nature [Internet] 1997 [cited 2014 Jan 21]; 389:607-10. Available from: http://www.ncbi.nlm.nih.gov/pubmed/9335501; PMID:9335501; http://dx.doi.org/10.1038/39329
18. Carattino MD, Sheng S, Bruns JB, Pilewski JM, Hughey RP, Kleyman TR. The epithelial Na^+ channel is inhibited by a peptide derived from proteolytic processing of its alpha subunit. J Biol Chem [Internet] 2006 [cited 2014 Feb 27]; 281:18901-7. Available from: http://www.ncbi.nlm.nih.gov/pubmed/16690613; PMID:16690613; http://dx.doi.org/10.1074/jbc.M604109200
19. Hu JC, Bengrine A, Lis A, Awayda MS. Alternative mechanism of activation of the epithelial na+ channel by cleavage. J Biol Chem [Internet] 2009 [cited 2014 Feb 27]; 284:36334-45. Available from: http://www.pubmedcentral.nih.gov/articlerender.fcgi?artid=2794749&tool=pmcentrez&rendertype=abstract; PMID:19858199; http://dx.doi.org/10.1074/jbc.M109.032870
20. Askwith CC, Benson CJ, Welsh MJ, Snyder PM. DEG/ENaC ion channels involved in sensory transduction are modulated by cold temperature. Proc Natl Acad Sci U S A [Internet] 2001 [cited 2014 Jul 2]; 98:6459-63. Available from: http://www.pubmedcentral.nih.gov/articlerender.fcgi?artid=33490&tool=pmcentrez&rendertype=abstract; PMID:11353858;http://dx.doi.org/10.1073/pnas.111155398
21. Awayda MS, Shao W, Guo F, Zeidel M, Hill WG. ENaC-membrane interactions: regulation of channel activity by membrane order. J Gen Physiol [Internet] 2004 [cited 2014 Jul 2]; 123:709-27. Available from: http://www.pubmedcentral.nih.gov/articlerender.fcgi?artid=2234566&tool=pmcentrez&rendertype=abstract; PMID:15148329; http://dx.doi.org/10.1085/jgp.200308983
22. Awayda MS. Specific and nonspecific effects of protein kinase C on the epithelial Na (+) channel. J Gen Physiol [Internet] 2000 [cited 2014 Feb 25]; 115:559-70. Available from: http://www.pubmedcentral.nih.gov/articlerender.fcgi?artid=2217227&tool=pmcentrez&rendertype=abstract; PMID:10779314; http://dx.doi.org/10.1085/jgp.115.5.559
23. Vogel C, Marcotte EM. Insights into the regulation of protein abundance from proteomic and transcriptomic analyses. Nat Rev Genet [Internet] 2012 [cited 2014 Mar 23]; 13:227-32. Available from: http://www.pubmedcentral.nih.gov/articlerender.fcgi?artid=3654667&tool=pmcentrez&rendertype=abstract; PMID:22411467
24. Pisitkun T, Shen R-F, Knepper MA. Identification and proteomic profiling of exosomes in human urine. Proc Natl Acad Sci U S A [Internet] 2004 [cited 2014 Jul 17]; 101:13368-73. Available from: http://www.pubmedcentral.nih.gov/articlerender.fcgi?artid=516573&tool=pmcentrez&rendertype=abstract; PMID:15326289; http://dx.doi.org/10.1073/pnas.0403453101
25. Canessa CM, Schild L, Buell G, Thorens B, Gautschi I, Horisberger JD, Rossier BC. Amiloride-sensitive epithelial Na^+ channel is made of three homologous subunits. Nature [Internet] 1994 [cited 2014 Mar 4]; 367:463-7. Available from: http://www.ncbi.nlm.nih.gov/pubmed/8107805; PMID:8107805; http://dx.doi.org/10.1038/367463a0
26. Schild L, Canessa CM, Shimkets RA, Gautschi I, Lifton RP, Rossier BC. A mutation in the epithelial sodium channel causing Liddle disease increases channel activity in the Xenopus laevis oocyte expression system. Proc Natl Acad Sci U S A [Internet] 1995 [cited 2014 Mar 4]; 92:5699-703. Available from: http://www.pubmedcentral.nih.gov/articlerender.fcgi?artid=41764&tool=pmcentrez&rendertype=abstract; PMID:7777572; http://dx.doi.org/10.1073/pnas.92.12.5699
27. Awayda MS, Shao W, Guo F, Zeidel M, Hill WG. ENaC-membrane interactions: regulation of channel activity by membrane order. J Gen Physiol [Internet] 2004 [cited 2014 Jul 15]; 123:709-27. Available from: http://jgp.rupress.org/content/123/6/709.long; PMID:15148329; http://dx.doi.org/10.1085/jgp.200308983
28. Palmer LG, Frindt G. Gating of Na channels in the rat cortical collecting tubule: effects of voltage and membrane stretch. J Gen Physiol [Internet] 1996 [cited 2014 Oct 16]; 107:35-45. Available from: http://www.pubmedcentral.nih.gov/articlerender.fcgi?artid=2219247&tool=pmcentrez&rendertype=abstract; PMID:8741729; http://dx.doi.org/10.1085/jgp.107.1.35
29. Hughey RP, Bruns JB, Kinlough CL, Harkleroad KL, Tong Q, Carattino MD, Johnson JP, Stockand JD, Kleyman TR. Epithelial sodium channels are activated by furin-dependent proteolysis. J Biol Chem [Internet] 2004 [cited 2014 Jul 21]; 279:18111-4. Available from: http://www.ncbi.nlm.nih.gov/pubmed/15007080; PMID:15007080; http://dx.doi.org/10.1074/jbc.C400080200
30. Buhl KB, Friis UG, Svenningsen P, Gulaveerasingam A, Ovesen P, Frederiksen-Møller B, Jespersen B, Bistrup C, Jensen BL. Urinary plasmin activates collecting duct ENaC current in preeclampsia. Hypertension [Internet] 2012 [cited 2014 Jul 21]; 60:1346-51. Available from: http://www.ncbi.nlm.nih.gov/pubmed/22987920; PMID:22987920;http://dx.doi.org/10.1161/HYPERTENSIONAHA.112.198879
31. Patel AB, Chao J, Palmer LG. Tissue kallikrein activation of the epithelial Na channel. Am J Physiol Renal Physiol [Internet] 2012 [cited 2014 Jul 21]; 303:F540-50. Available from: http://ajprenal.physiology.org/content/303/4/F540; PMID:22622459; http://dx.doi.org/10.1152/ajprenal.00133.2012
32. Sheng S, Carattino MD, Bruns JB, Hughey RP, Kleyman TR. Furin cleavage activates the epithelial Na^+ channel by relieving Na^+ self-inhibition. Am J Physiol Renal Physiol [Internet] 2006 [cited 2014 Jul 23]; 290:F1488-96. Available from: http://www.ncbi.nlm.nih.gov/pubmed/16449353; PMID:16449353; http://dx.doi.org/10.1152/ajprenal.00439.2005
33. Nesterov V, Dahlmann A, Bertog M, Korbmacher C. Trypsin can activate the epithelial sodium channel (ENaC) in microdissected mouse distal nephron. Am J Physiol Renal Physiol [Internet] 2008 [cited 2014 Mar 17]; 295:F1052-62. Available from: http://www.ncbi.nlm.nih.gov/pubmed/18653483; PMID:18653483; http://dx.doi.org/10.1152/ajprenal.00031.2008
34. Harvey BJ. Energization of sodium absorption by the H(+)-ATPase pump in mitochondria-rich cells of frog skin. J Exp Biol [Internet] 1992 [cited 2014 Jul 29]; 172:289-309. Available from: http://www.ncbi.nlm.nih.gov/pubmed/1491227; PMID:1491227
35. Lide DR, editor. Mean activity coefficients of electrolytes as a function of concentration. In CRC Handbook of Chemistry and Physics [Internet]. CRC Press: Boca Raton, FL; 2014. Available from: http://www.hbcpnetbase.com/
36. Stoddard JS, Helman SI. Dependence of intracellular Na^+ concentration on apical and basolateral membrane Na^+ influx in frog skin. Am J Physiol [Internet] 1985 [cited 2014 Jul 24]; 249:F662-71. Available from: http://www.ncbi.nlm.nih.gov/pubmed/3877468; PMID:3877468
37. Rick R, Dörge A, von Arnim E, Thurau K. Electron microprobe analysis of frog skin epithelium: evidence for a syncytial sodium transport compartment. J Membr Biol [Internet] 1978 [cited 2014 Jul 24]; 39:313-31. Available from: http://www.ncbi.nlm.nih.gov/pubmed/641981; PMID:641981; http://dx.doi.org/10.1007/BF01869897
38. Nagel W, Garcia-Diaz JF, Armstrong WM. Intracellular ionic activities in frog skin. J Membr Biol [Internet] 1981 [cited 2014 Jul 24]; 61:127-34. Available from: http://www.ncbi.nlm.nih.gov/pubmed/6974243; PMID:6974243;http://dx.doi.org/10.1007/BF02007639
39. Solenov EI. Cell volume and sodium content in rat kidney collecting duct principal cells during hypotonic shock. J Biophys [Internet] 2008 [cited 2014 Jul 28]; 2008:420963. Available from: http://www.pubmedcentral.nih.gov/articlerender.fcgi?artid=2809319&tool=pmcentrez&rendertype=abstract; PMID:20107575; http://dx.doi.org/10.1155/2008/420963
40. Swayne LA, Bourinet E. Voltage-gated calcium channels in chronic pain: emerging role of alternative splicing. Pflugers Arch [Internet] 2008 [cited 2014 Jan 21]; 456:459-66. Available from: http://www.ncbi.nlm.nih.gov/pubmed/18389277; PMID:18389277;http://dx.doi.org/10.1007/s00424-007-0390-4
41. Bell TJ, Thaler C, Castiglioni AJ, Helton TD, Lipscombe D. Cell-specific alternative splicing increases calcium channel current density in the pain pathway. Neuron [Internet] 2004 [cited 2014 Mar 18]; 41:127-38. Available from: http://www.ncbi.nlm.nih.gov/pubmed/14715140; PMID:14715140; http://dx.doi.org/10.1016/S0896-6273(03)00801-8
42. McCormack K, McCormack T, Tanouye M, Rudy B, Stühmer W. Alternative splicing of the human Shaker K^+ channel beta 1 gene and functional expression of the beta 2 gene product. FEBS Lett [Internet] 1995 [cited 2014 Mar 18]; 370:32-6. Available from: http://www.ncbi.nlm.nih.gov/pubmed/7649300; PMID:7649300; http://dx.doi.org/10.1016/0014-5793(95)00785-8
43. Bengrine A, Li J, Hamm LL, Awayda MS. Indirect activation of the epithelial Na^+ channel by trypsin. J Biol Chem [Internet] 2007 [cited 2014 Mar 17]; 282:26884-96. Available from: http://www.jbc.org/content/282/37/26884.long; PMID:17627947; http://dx.doi.org/10.1074/jbc.M611829200
44. Awayda MS. Regulation of the Epithelial Na^+ Channel by Membrane Tension. J Gen Physiol [Internet] 1998 [cited 2014 Jul 23]; 112:97-111. Available from: http://jgp.rupress.org/content/112/2/97?ijkey=673bc41c3b2fcfc28b87ac15dfab4c673adafc2a&keytype2=tf_ipsecsha; PMID:9689021; http://dx.doi.org/10.1085/jgp.112.2.97
45. Berman JM, Awayda MS. Redox artifacts in electrophysiological recordings. Am J Physiol Cell Physiol [Internet] 2013 [cited 2014 Jan 29]; 304:C604-13. Available from: http://www.ncbi.nlm.nih.gov/pubmed/23344161; PMID:23344161; http://dx.doi.org/10.1152/ajpcell.00318.2012
46. Zhou H, Yuen PST, Pisitkun T, Gonzales PA, Yasuda H, Dear JW, Gross P, Knepper MA, Star RA. Collection, storage, preservation, and normalization of human urinary exosomes for biomarker discovery. Kidney Int [Internet] 2006 [cited 2014 Jul 10]; 69:1471-6. Available from: http://www.pubmedcentral.nih.gov/articlerender.fcgi?artid=2276656&tool=pmcentrez&rendertype=abstract; PMID:16501490
47. Rambaldi D, Ciccarelli FD. FancyGene: dynamic visualization of gene structures and protein domain architectures on genomic loci. Bioinformatics [Internet] 2009 [cited 2014 Feb 10]; 25:2281-2. Available from: http://www.pubmedcentral.nih.gov/articlerender.fcgi?artid=2734320&tool=pmcentrez&rendertype=abstract; PMID:19542150; http://dx.doi.org/10.1093/bioinformatics/btp381
48. Chalfant ML, Denton JS, Langloh AL, Karlson KH, Loffing J, Benos DJ, Stanton BA. The NH(2) terminus of the epithelial sodium channel contains an endocytic motif. J Biol Chem [Internet] 1999 [cited 2014 Mar 18]; 274:32889-96. Available from: http://www.ncbi.nlm.nih.gov/pubmed/10551853; PMID:10551853; http://dx.doi.org/10.1074/jbc.274.46.32889